

# REFRACTORIES IN HEATING UNITS

## MATERIAL SUBSTANCE COMPOSITION AND MICROSTRUCTURE OF THE CERAMIC HEARTH OF BLAST FURNACE NO. 6 EVRAZ NTMK AFTER SERVICE. PART 1. REFRACTORY MINERAL COMPOSITION

V. A. Perepelitsyn,<sup>1</sup> K. G. Zemlyanoi,<sup>1,3</sup> V. M., Ust'yantsev,<sup>1</sup> K. V. Mironov,<sup>2</sup>  
A. A. Forshev,<sup>2</sup> F. P. Nikolaev,<sup>2</sup> and D. V. Sushnikov<sup>2</sup>

Translated from *Novye Ogneupory*, No.5, pp. 41 – 47, May, 2022.

*Original article submitted March 23, 2022.*

Results are presented for a comprehensive study of the chemical and material composition, as well as the macrostructure, of refractory samples after over 14 years service in a blast furnace hearth with a useful volume of 2200 m<sup>3</sup>. Sample carbon content is determined using a comprehensive method. Zinc-containing phase formation is established in both the ceramic nozzle area oxide refractories and within the carbon lining of the furnace tuyere zone and hearth. Furnace refractory wear is complex, predominantly by a thermochemical mechanism, and a slow rate due to garnish formation containing refractory compounds.

**Keywords:** blast furnace (BF), ceramic hearth, carbon lining, wear resistance, zincite, ganite, willemite.

Currently in view of intensification of high-temperature processes the campaign duration for contemporary blast furnaces (BF) is governed to a significant extent by hearth and bottom wear resistance [1 – 5]. It is also well known that a considerable part of a BF campaign operates not on the original lining but on its working surface formed by a refractory skull. The skull substance composition and properties have been the object of study by overseas and domestic authors [1 – 10]. The majority of publications is devoted to studying a BF skull, melting cast iron with the iron ore raw material used traditionally with a relatively low titanium content [2 – 7]. In this case the physicochemical wear mechanism for the hearth lining itself has not been studied adequately.

This article contains the first results of comprehensive materials science investigation of a new generation of refractories for lining a hearth, tuyere zone, and ceramic housing after 14 years of operation in the BF No. 6 with a considerable useful volume; some aspects of systematic study of the skull formed within this BF during the same campaign have been published previously [1].

### RESEARCH OBJECTS

EVRAZ NTMK BF No. 6 with a useful volume of 2200 m<sup>3</sup> (hearth diameter 9700 mm, two cast iron notches, 22 air tuyeres) was blown in after reconstruction in 2004 and blown down for subsequent repair in 2018. For this period 27, 950 thousand tons of finished vanadium-containing cast iron was melted. The average cast iron chemical composition, wt. %: Fe 94.1, Ti 0.14, V 0.496, Mn 0.38, C 4.6, Si 0.08, S 0.024, P 0.05.

After blowing down the furnace and cooling with air and water the lining and skull were broken down by means of a machine lining breakage with a hydraulic hammer and removed from the furnace. In this case samples were selected from the hearth, tuyere zone, and shoulders. In all four specimens of the hearth lining were presented for study: from the main carbon lining and ceramic nozzle. Points for lining specimen sample selection of FB No. 6 and are shown in Fig. 1.

Specimens O1 and O3 were represented by degenerated carbon lining blocks selected from points +9550 and +9500 mm respectively, located above the slag and cast iron tap holes. Specimen O4 selected in the region of cast iron tap hole No. 2 (level +9300 mm) was part of a layered carbon

<sup>1</sup> FGAOU PO Ural Federal University, Ekaterinburg, Russia.

<sup>2</sup> AO EVRAZ NTMK, Nizhnii Tagil, Russia.

<sup>3</sup> kir77766617@yandex.ru

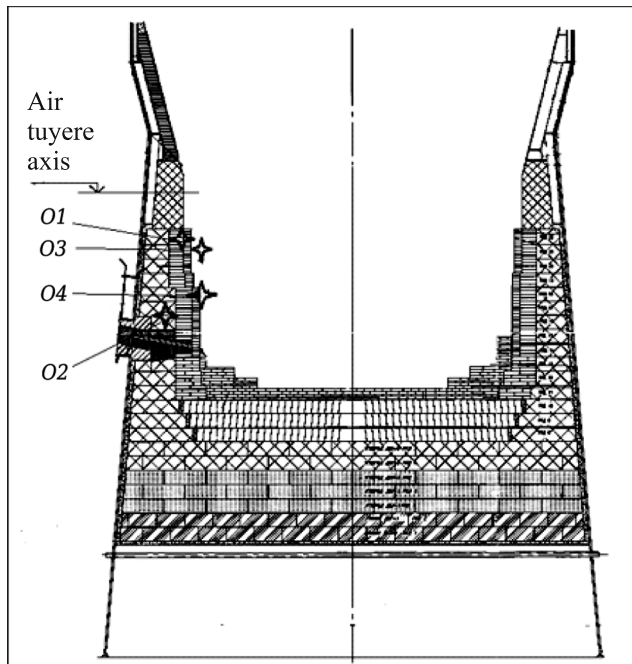


Fig. 1. Layout of a selection of refractory samples *O1*, *O2*, *O3*, *O4* over the height of EVRAZ NTMK BF No. 6.

block. Specimen *O2* is represented by changed graphite refractory selected from mark +9100 mm.

The hearth ceramic nozzle was prepared from dense aluminosilicon carbide objects grade MTZST-1 and blocks grade MTZST-ZH produced by Mayerton (CPR), the carbon lining of the hearth was prepared from carbon blocks produced domestically (Chelyabinsk electrode plant). The chemical composition and physical properties of imported refractories before service are provided in Table 1 and the mineral composition is provided in Table 2.

TABLE 1. Alumina-Silicon Carbide Ceramic Nozzle Object Chemical Composition and Properties

Index	MTZST-1 object	MTZST-ZH block
Content, wt. %:		
Al <sub>2</sub> O <sub>3</sub>	≥75.0	≥70.0
SiO <sub>2</sub>	≤14.0	≤21.0
SiC	9.0	8.0
Fe <sub>2</sub> O <sub>3</sub>	≤1.0	≤1.0
Apparent density, g/cm <sup>3</sup>	≥3.0	≥3.0
Ultimate strength, MPa:		
in compression	≥100	≥80
in bending	≥18	≥16
Open porosity, %	≤16	≤16
Refractoriness, °C	≥1790	≥1790
Temperature for stat of deformation under load of 0.2 MPa, °C	≥1700	≥1680
Thermal conductivity, W/(m·K)	5.0	5.0
LTEC, %	0 – 0.5	0 – 0.5
Thermal stability, heat exchanges	≥30	—

## RESEARCH PROCEDURE

The chemical composition of the test materials was determined in an x-ray fluorescence energy-dispersion spectrometer ARL QUANT'X (Thermo Scientific, USA) using a UniQUANT program (Rh  $K_{\alpha}$ -radiation, tube power 50 W, voltage range 4 – 50 kV with a step of 1 kV, current range 0 – 1.98 mA with a step of 0.2 mA, Si (Li) detector, energy resolution 150 eV).

TABLE 2. Alumina-Silicon Carbide Ceramic Nozzle Object Mineral Composition

Mineral	Melting temperature, °C	Mineral composition, %*1			
		MTZST-1 object		MTZST-ZH block	
		<i>a</i>	<i>b</i>	<i>a</i>	<i>b</i>
Corundum	2050	40.3	36 – 40	16.5	15 – 18
Mullite 3Al <sub>2</sub> O <sub>3</sub> ·2SiO <sub>2</sub>	1910	49.7	46 – 50	74.5	68 – 72
Glass R <sub>2</sub> O·RO·nSiO <sub>2</sub> *2	—	—	3 – 5	—	5 – 7
Silicon carbide α-SiC	2830*3	9.0	8 – 10	8.0	68
Magnesite Fe <sub>3</sub> O <sub>4</sub>	1580	1.0	0.6 – 1.0	1.0	0.3 – 0.7
Impurities (Si, SiO <sub>2</sub> , etc.)	—	—	0.2	—	Not det.

\*1 *a* is calculated equilibrium composition; *b* is actual mineral (phase).

\*2 R<sub>2</sub>O — K<sub>2</sub>O, Na<sub>2</sub>O; RO — CaO + MgO.

\*3 Sublimation temperature shown, °C.

The change in phase composition and weight on heating and melting temperature were determined by a thermogravimetric method in a differential scanning derivatograph STA 449 F3 Jupiter (Netzsch-Gerätebau GmbH) using a Proteus Analysis 5.2 program by the procedure DIN 51004:1994 (Determination of melting temperatures of crystalline materials using differential thermal analysis). The error for the method in determining melting temperature was  $\pm 3\%$ .

**TABLE 3.** Refractory Reaction Zone Chemical Composition (After Calcining in Air at 1000°C)

Component	Component content, wt.%, in specimen (see Fig. 1)			
	<i>O1</i>	<i>O2</i>	<i>O3</i>	<i>O4</i>
Fe	0.446	5.32	0.667	4.14
Si	11.11	3.36	30.68	76.74
Ti	0.666	0.237	1.99	1.25
Zn	65.15	82.23	23.15	0.833
Ca	0.236	0.587	0.858	1.22
Mn	0.0215	0.0603	0.0495	0.0493
K + Na	0.114	0.424	0.813	2.47
V	—	0.077	0.045	0.241
Al	19.37	5.21	40.22	9.98
S	0.54	—	—	0.907
Co	—	0.052	0.0204	0.035
Cu	—	—	—	0.166
Pb	1.13	0.599	0.162	0.0115
Cr	—	—	—	0.0734
Ba	0.00336	—	0.066	—
REE (Y, Ce)	0.11	0.1226	0.3428	0.1662
Mo + W	0.89	1.57	0.46	0.0137
Ni	—	—	—	0.0311
Zr	0.114	—	0.377	0.307
Cl + I + Br	—	—	—	1.3198
Bi	0.0626	0.139	—	—
P	—	—	0.201	—
C <sub>free</sub>	—	—	—	43
SiC	—	—	—	42
SiO <sub>2</sub>	15.81	3.52	35.76	7.76
Al <sub>2</sub> O <sub>3</sub>	27.29	8.17	47.34	3.43
FeO	0.439	5.89	0.48	0.88
CaO	0.257	0.668	0.638	0.604
MgO	—	0.58	—	—
ZnO	53.56	77.52	12.89	0.306
Sum	99.79	97.54	99.36	99.14
Other micro-impurities	0.21	2.46	0.64	0.86

X-ray phase analysis (XPA) was conducted in a Miniflex 600 diffractometer with a rotating anode (Cu  $K_{\alpha}$ -radiation,  $\lambda = 1,541862 \text{ \AA}$ , recording range 3.00 – 60.00 deg, scanning step 0.02 deg, Rigaku — Carl Zeiss, Japan) with program control and selection of Miniflex guidance data and a PDXL Basic treatment package. Identification of the diffraction maxima was conducted using a JSPDS data bank, semi quantitative evaluation of the phase content was performed using corundum number (Reference Intensity Ratio) by the Chung method [11].

## RESULTS AND DISCUSSION

The chemical composition of the refractory test samples after service is provided in Table 3. The broad range of the main component (substances) content is seen represented by a very complex multicomponent system Fe–C–FeO–Fe<sub>2</sub>O<sub>3</sub>–CaO–MgO–Al<sub>2</sub>O<sub>3</sub>–TiO<sub>2</sub>–ZnO–V<sub>2</sub>O<sub>5</sub>–SiO<sub>2</sub>. The content of individual elements was determined instrumentally. A considerable number of impurity elements should be noted falling into the BF with iron raw material, coke, and fluxes (Table 4).

Comparison of data provide in Tables 3 and 4 shows a very high zinc concentration in specimens *O1*–*O3* (23.2 – 82.2 wt.%), an insignificant content of slag oxides (CaO and MgO <1.0 wt.%), and a reduction in the amount of Al<sub>2</sub>O<sub>3</sub> within a lining during service by several factors (in specimen *O1* by almost an order of magnitude). Specimen *O4* is distinguished from others predominantly by silica composition; it contains 81.7 wt.% SiO<sub>2</sub>. In all specimens a relatively low Fe content was established that points to a lack of iron migration from melts into refractory.

**Fig. 2.** Refractory specimens collected from BF No. 6 hearth: *a*) specimen *O1*, part of lining block from mark +9500 mm; *b*) specimen *O2*, part of graphitized block of 1-st row; *c*) specimen *O3*, regenerated part of carbon block from mark +9500 mm; *d*) specimen *O4*, carbon block layered part from mark +9300 mm, cast iron tap-hole No. 2.

### Specimen macro characteristics

Specimens selected for comprehensive study are shown in Fig. 2. Careful examination of specimens *O1* and *O3* show presence within their surface and within the plane of a section of finely dispersed carbon (possibly sooty) which is not washed out even by a stream of water. The volumetric saturation with carbon during service causes transfer of a light grey specimen color into dark grey. In specimens *O2* and *O4* carbon is represented by two varieties: finely dispersed (sooty) and finely crystalline (graphite).

Within sections of specimens *O1* and *O3* there a fine (up to 1.0 – 1.5 mm) cracks entirely filled with refractory light-grey substance, i.e., zincite ZnO ( $T_m = 1975^\circ\text{C}$ ). the texture of these specimens is mainly uniform, without visible boundaries between filler grains (fraction >0.01 mm) and matrix (<0.1 mm).

Specimens do not exhibit magnetic permeability, do not contain spots of cast iron, which points to the absence marked capillary infiltration of molten metal within the refractory volume. Due to additional sintering and impregnation by reagents of the furnace space specimen open porosity decreases from 16 to 6.1% and apparent density increases to

3.95 g/cm<sup>3</sup>. Apparently the increase in density is connected with presence of zincite having an apparent density of 5.7 g/cm<sup>3</sup>.

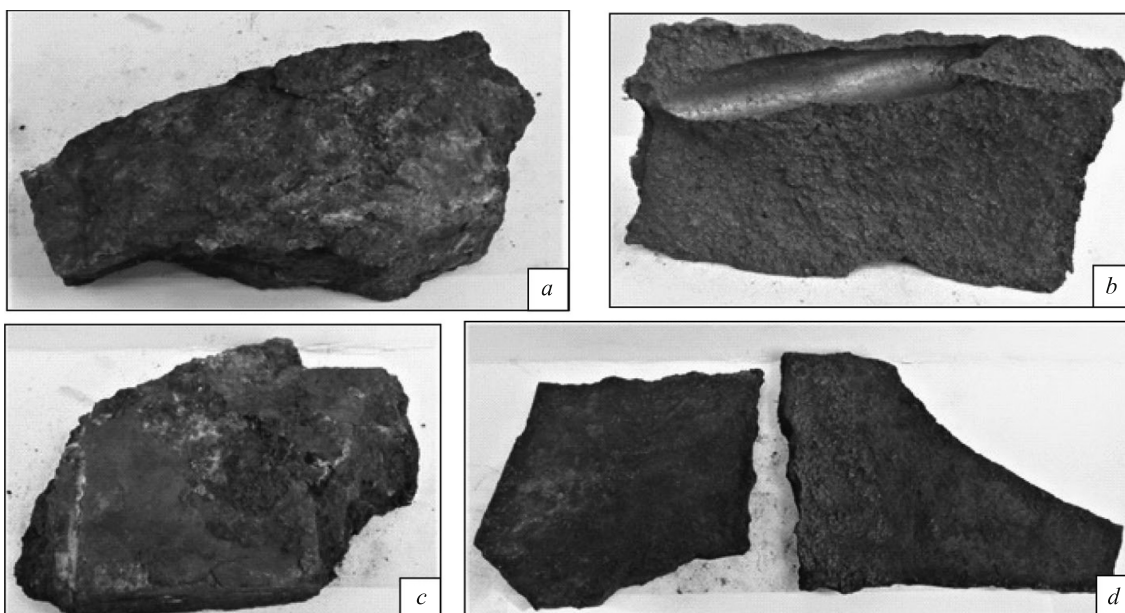
Visual examination also shows complete absence of macro-zonality in all of the specimens studied. Specimens O1 and O3 have high mechanical strength. Carbon blocks

**TABLE 4.** Blast Furnace Melting Charge Material Chemical Composition

Material	Content, wt.%														Basicity
	Fe	FeO	Fe <sub>2</sub> O <sub>3</sub>	V <sub>2</sub> O <sub>5</sub>	MgO	S	Zn	TiO <sub>2</sub>	Mn	CaO	SiO <sub>2</sub>	P	Al <sub>2</sub> O <sub>3</sub>	Cr	
Kachkanar GOK agglomerate	54.1	9.4	66.9	0.527	2.57	0.017	0.012	2.51	0.17	11.0	4.7	0.006	2.58	0.057	2.33
Kachkanar GOK pellets	61.1	3.2	83.9	0.588	2.53	0.004	0.013	2.75	0.17	1.2	3.8	0.006	2.53	0.52	0.31
Vysokogor GOK iron-flux	51.9	10.4	62.6	0.659	3.35	0.043	0.088	1.79	0.45	12.8	5.5	0.036	2.58	0.111	2.32
Steel gabarite blast furnace deposit* <sup>1</sup>	60.2	18.4	—	0.772	5.51	0.066	0.035	0.84	1.83	11.7	7.3	0.153	2.24	0.23	1.59
RM UPoSh metal product* <sup>2</sup>	72.5	12.3	—	0.385	2.91	0.148	—	2.10	0.61	8.0	6.7	0.055	2.83	—	1.19
RM UPoSh metal addition	88.8	1.6	—	0.66	0.84	0.046	—	0.25	0.33	2.5	2.2	0.05	0.87	—	1.14
VSPS metal fines* <sup>2</sup> (mixture)	83.0	—	—	6.204	0.40	—	—	2.25	2.60	0.5	3.3	0.011	—	—	0.16
Dry MV metal product (Sukhoi Log)	88.3	—	—	4.10	0.23	—	—	1.39	1.73	0.3	2.1	0.013	—	—	0.15
EVRAZ NTMK coke production ash	—	—	20.2	—	1.1	—	—	—	—	5.1	48.1	0.30	20.4	—	0.10
BF No. 6 slag [12]	—	1.10	—	0.24	12.0	—	—	9.99	0.4	32.9	28.4	—	15.7	—	—
BF No. 6 cast iron [12]	—	—	—	V	—	0.023	—	Ti	0.24	—	Si	—	—	—	1.14
				0.423				0.16			0.11				

\*<sup>1</sup> Additionally contains 0.1 wt.% Na<sub>2</sub>O, 0.08 wt.% K<sub>2</sub>O, and 0.003 wt.% Pb.

\*<sup>2</sup> UPOSh is dump slag preparation section; VSPS is vanadium-containing slag preparation section.



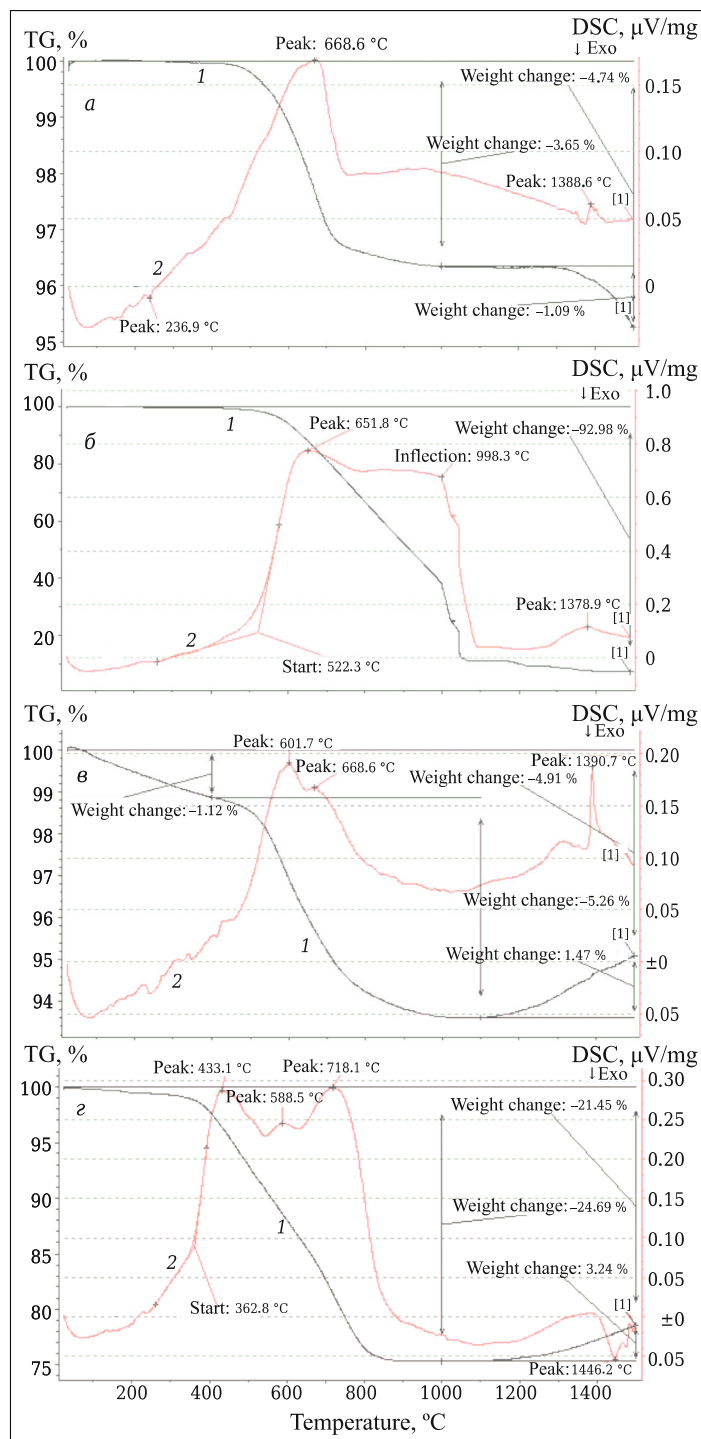


**Fig. 3.** Refractory specimen thermograms in air atmosphere: 1) weight loss (TG) curve; 2) thermal effect curve (DSC); a – d) specimens O1, O2, O3, and O4 respectively.

also do not have macro-zonality but they exhibit a layered texture with different layer density with thickness from several millimeters to 15 cm or more. Layers are densely and strongly sintered into a monolith and differ in macro porosity and color.

### Determination of specimen carbon content

It is well known that carbon within refractories before and after service may be present in a bonded form (carbides, oxycarbides, carbonates) and in elemental form (C) with a different degree of crystalline structure ordering: from almost x-ray amorphous soot to clearly crystalline graphite. In this case coke before development of an atomic structure (close ordering) occupies an intermediate position. An important diagnostic parameter of the solid carbon with a different developed crystalline structure is the temperature for the start of oxidation in air, increasing with development of its perfection [14]. Among traditional methods for studying carbon mineral substance, (chemical, x-ray phase, metallographic, infrared spectroscopy, etc.) the most effective is thermogravimetric (or differential calorimetry, i.e., DSC) based on synchronous recording of the rate in temperature change and sample weight on heating within a prescribed medium. Weight loss curves (TG), and thermal effects (DSC) of four test samples studied on heating in air at a rate of 10°C/min in the range 20 – 1500°C are shown in Fig. 3.

Weight loss for specimen O1 commences from 400°C and proceeds in two stages; in the range 400 – 1200°C with a maximum thermal effect at 669°C, connected with carbon oxidation (weight loss 3.65%) and possibly zinc, and a small exothermic effect in the range 1300 – 1500°C connected with glass phase and crystalline mullite breakdown possibly enriched with zinc at 1389°C (weight loss 1.09%). The amount of free carbon within a specimen is 3.65%.

Thermal effects in specimen O2 commence from 200°C and are accompanied by a broad exothermic effect with a maximum 652°C, connected with carbon and possibly zinc oxidation, and some exothermic effect in the range 1300 – 1500°C as a result of glass phase devitrification and mullite crystallization, i.e., an exothermic effect at 1379°C. The extensive effect of carbon oxidation is due to presence within a specimen of oxide and/or metallic phase that during carbon combustion forms an oxide film at its surface, slowing down the oxidation process. The amount of free carbon in a specimen is 93.0%.

Thermal effects in specimen O3 commence from 200°C and are accompanied by a broad exothermic effect with maxima at 602 and 669°C, reflecting successive processes of zinc, carbon, coke, and graphite oxidation. Starting at 1100°C another exothermic effect develops accompanied by a weight increase of 1.47% and a clearly expressed exothermic effect in the range 1300 – 1500°C due to carbide ( $\text{Fe}_3\text{C}$ ,  $\text{SiC}$ ) phase oxidation. The amount of free carbon within a specimen is 5.26%.

Thermal effects in specimen O4 commence from 200°C and are accompanied by a broad exothermic effect with a maximum in the range 433 – 718°C connected with oxida-

TABLE 5. Test Specimen Phase Composition (According to XPA Data)

Phase	Phase content, wt.%, in specimen					
	O1	O2*1		O3	O4*1	
		a	b		a	b
Zincite ZnO	36	—	26	—	—	—
Ganite ZnAl <sub>2</sub> O <sub>4</sub>	7	—	—	—	—	—
Willemite Zn <sub>2</sub> SiO <sub>4</sub>	11	3	1.6	3	—	—
Ferrous mullite 3(Al,Fe) <sub>2</sub> O <sub>3</sub> ·2(Si)O <sub>3</sub>	22	—	—	63	—	—
Ferrous corundum (Al,Fe) <sub>2</sub> O <sub>3</sub>	24	—	—	—	—	—
Ferrous zincite (Zn,Fe)O	—	49	—	29	—	—
Ferrous ganite Zn(Al <sub>1,4</sub> Fe <sub>0,6</sub> )O <sub>4</sub>	—	48	—	—	—	—
Hercynite zincate (Zn <sub>0,4</sub> Fe <sub>0,52</sub> Al <sub>0,08</sub> )(Fe <sub>0,09</sub> Al <sub>1,91</sub> O <sub>4</sub> )	—	—	—	2	—	—
Graphite	—	—	69	—	43	13
Silicon carbide*2	—	—	—	—	50	53
Coghennite Fe <sub>3</sub> C*3	—	—	4	—	1	—
Braunmullerite Ca <sub>2</sub> Fe <sub>0,95</sub> Al <sub>0,95</sub> Mg <sub>0,05</sub> Si <sub>0,05</sub> O <sub>5</sub>	—	—	—	—	3	—
Pyrope (Mg <sub>0,92</sub> Fe <sub>0,05</sub> Ca <sub>0,03</sub> ) <sub>3</sub> Al <sub>2</sub> (SiO <sub>4</sub> ) <sub>3</sub>	—	—	—	—	3	—
Quartz	—	—	—	—	—	34

\*1 a) calculated equilibrium composition; b) actual mineral (phase).

\*2 Synonym — cementite (material science).

\*3 In high-temperature modification geology (hexagonal syngony) called moissanite.

tion of sooty carbon, coke, and graphite, and some endothermic effect at 1446°C caused by melting of amorphous phase. The amount of free carbon in a specimen is 24.69%.

The temperature for the start of melting for all specimens in a protective atmosphere is above 1600°C.

### Specimen quantitative XPA

XPA results for six of the samples studied are provided in Table 5. For analysis of specimens O2 and O4 there was use of two varieties of layers (O2-a, O2-b, O4a, O4-b) differing in microstructure. It is seen from Table 5 that specimen O1 and O3 with respect to phase composition are similar to refractory of high-alumina objects represented by mullite and corundum, containing iron oxide in the form of isomorphic impurities. Specimens O2 and O4 differ considerably from specimen O1 and O3 predominantly in carbon content represented by Si-C system phases: graphite and silicon carbide. Specimen O4 contains about one third quartz within a gray layer of a block. Results of XPA also show that zinc compound oxidation, represented by zincite ZnO, gahnite ZnAl<sub>2</sub>O<sub>4</sub>, and zinc hercynite (Fe,Zn)Al<sub>2</sub>O<sub>4</sub>, are contained in the form of a solid solution of FeO and Fe<sub>2</sub>O<sub>3</sub>.

### Specimen quantitative petrographic analysis

An important disadvantage of XPA is the impossibility of obtaining information about the content in test specimen of

x-ray amorphous specimen, in particular glass phase and carbon in the form of soot, coke, and glassy carbon. This disadvantage is overcome by combined use with XPA of more effective thermography methods, i.e., the weight content of all forms of carbon including finely dispersed soot and petrography (all forms of carbon apart from soot).

The actual mineral composition of the test specimens after service in a BF and the main XPA and thermogravimetric results, overall and local chemical analyses and mineral content (according to optical microscopy data in reflected light) are provided in Table 6. Comparison of results of quantitative determination of the XPA mineral composition (see Table 5) and microscopy (see Table 6) makes it possible to obtain more complete information about the these specimen actual composition, including the content and mutual location of amorphous phases.

With respect to mineral composition the original refractories are separated into two groups: corundum mullite silicon carbide (specimen O1 and O3) relating to the Al<sub>2</sub>O<sub>3</sub>-2SiO<sub>2</sub>-SiC system, and carbon-containing (unfired specimen O2 and O4) described by the system Al<sub>2</sub>O<sub>3</sub>-2SiO<sub>2</sub>-SiC-C. In all specimens secondary x-ray amorphous carbon (soot) was diagnosed in an amount of 3 – 5%. Important secondary minerals, formed as a results of take-up of substances from the BF workspace and their chemical interaction with original refractory phases are four zinc com-

TABLE 6. Test Specimen Mineral (Phase) Composition

Phase	$T_m$ , °C	Phase content, wt.%, in specimen			
		O1	O2	O3	O4
Normal corundum (Al,Ti) <sub>2</sub> O <sub>3</sub>	2050	25.0	—	46.2	18.4
Mullite 3Al <sub>2</sub> O <sub>3</sub> ·2SiO <sub>2</sub>	1910	4.3	—	12.6	—
Silicon carbide	>2600* <sup>1</sup>	12.8	—	18.8	33.6
Zincite ZnO	1975	35.4	2.0	6.2	—
Carbon (coke and graphite)	>3500* <sup>1</sup>	4.8	63.1	3.7	32.9
Ganite ZnAl <sub>2</sub> O <sub>4</sub>	1950	7.0	1.3	3.3	—
Willemite Zn <sub>2</sub> SiO <sub>4</sub>	1512	9.3	1.6	4.1	—
Glass (lechatelierite)* <sup>2</sup>	—	1.4	—	1.3	—
Zinc metal	420	—	24.1	3.8	—
Cementite (coghennite) Fe <sub>3</sub> C	1600	—	8.0	—	—
Quartz	1723	—	—	—	15.1

\*<sup>1</sup> Sublimation temperature shown, °C.

\*<sup>2</sup> Base — SiO<sub>2</sub> (from SiC).

pounds: zinc metal, zinc oxide, zinc silicate, i.e., willemite Zn<sub>2</sub>SiO<sub>4</sub>, and zinc spinel gahnite ZnAl<sub>2</sub>O<sub>4</sub>. The overall content of zinc-containing phases within specimen O1 exceeds 51%.

## REFERENCES

1. V. A. Perepelitsyn, K. G. Zemlyanoi, K. V. Mironov, et al., "Mineralogy and microstructure of skull versions in AO EVRAZ NTMK blast furnace No. 6," *Refract. Ind. Ceram.*, **61**(4), 364 – 373 (2020).
2. A. V. Gorokh and L. N. Rusakov, *Petrographic Analysis of Processes in Metallurgy* [in Russian], Metallurgiya, Moscow (1973).
3. D. Bergsma and R. J. Fruehan, "Fundamentals of titanium-rich scaffold formation in the blast furnace heath," *Ironmaking Conference Proceedings*, 297 – 312 (2001).
4. A. M. Koverzin, V. G. Shchinityn, A. V. Vashchenko, et al., "Study of glazing and lining of blast furnace hearth No. 2 AO EVRAZ 3SMK (Communication 1)," *Chern. Met. Byul. Nauch. Ekon. Inform.*, No. 8, 17 – 29 (2018).
5. A. M. Kaverzin, V. G. Shchinityn, A. V. Vashchenko, et al., "Study of glazing and lining of blast furnace hearth No. 2 AO EVRAZ 3SMK (Communication 2)," *Chern. Met. Byul. Nauch. Ekon. Inform.*, No. 9, 9 – 24 (2018).
6. I. F. Kurunov, A. S. Bliznyukov, V. N. Titov, et al., "Study of the composition and structure of glazing the skull of BF hearth No. 6 NLMK (Communication 1)," *Chern. Met. Byul. Nauch. Ekon. Inform.*, **75**(6), 166 – 181 (2019).
7. I. É. Shepetovskii, A. G. Shalygin, M. R. Sadradinov, et al., "Study of the composition of the skull in a blast furnace hearth of the Kosogor metallurgical Plant smelting ferromanganese using shungite (Communication 1)," *Chern. Met. Byul. Nauch. Ekon. Inform.*, **75**(4), 432 – 447 (2019).
8. V. A. Perepeitsyn, A. S. Freidenburg, and I. N. Sorokin, "Some processes of skull formation in a blast furnace charge," *Ogneupory*, No. 2, 39042 (1976).
9. V. V. Filippov, V. S. Rudin, A. Yu. Chernavin, et al., "Study of skull formation during melting titanium magnetites of the Kachkanarsk GOK," *Stal'*, No. 5, 15 – 18 (2000).
10. V. A. Gostenin, S. K. Sibgatulin, A. L. Mavrov, et al., "Structure of carbonitride glazing formed in hearth and shoulder," *Stal'*, No. 2, 29 – 30 (2007).
11. C. R. Hubbard, E. H. Evans, and D. K. Smith, "The reference intensity ratio for computer simulated powder patterns," *J. Appl. Cryst.*, **169**(9), 169 – 174 (1976).